Extended Method for Adiabatic Mode Reordering

**CHRISTOFER S. TAUTERMANN,[1] ANDREAS F. VOEGELE,[1] THOMAS LOERTING,[1]
PETER KAPS,[2] KLAUS R. LIEDL[1]**

[1]*Institute of General, Inorganic and Theoretical Chemistry, University of Innsbruck,
Innrain 52a, A-6020 Innsbruck, Austria*
[2]*Department of Engineering Mathematics, Geometry and Computer Science,
Faculty of Civil Engineering and Architecture, University of Innsbruck,
Technikerstraße 13, A-6020 Innsbruck, Austria*

Abstract: The task of vibrational mode reordering is very important for reaction valley studies and for the determination of small curvature tunneling effects. An extended algorithm for adiabatic mode reordering is presented. It is based on the method introduced by Konkoli et al. [J Comput Chem 1997, 18, 1282], which is shown to suffer from numerical problems in the region of frequency-crossings and avoided crossings. One improvement is the use of cubic splines for the interpolation of the projected matrix of force constants, which allows larger step sizes between the discrete points along the reaction path, where vibrational analysis is performed. The main improvement is the use of perturbation theory to resolve crossings and avoided crossings. Within this theoretical framework it becomes clear why the method of the maximal overlap between the normal modes cannot work properly, as eigenvectors associated with nearby eigenvalues tend to become "wobbly". Thus a perturbative procedure is designed that is used for all cases where two harmonic frequencies approach each other and the overlap of the associated normal modes is of no practical use. Advantages of the new procedure are the use of larger step sizes along the minimum energy path and the much more reliable resolution of mode-crossings and avoided crossings independent of the systems symmetry. In addition to that it is shown that one should be very cautious in all computational situations when working with eigenvectors associated with nearby eigenvalues.

© 2003 Wiley Periodicals, Inc.   J Comput Chem 24: 386–395, 2003

Key words: vibrational normal modes; reaction valley studies; perturbation theory

Introduction

When investigating a chemical reaction quantum mechanically, the stationary points (i.e., the minima and the transition state) as well the reaction valley connecting them are of big interest. The stationary points are characterized by a zero gradient and 3N-6 normal modes, when performing a vibrational analysis for a non-linear molecule with N atoms.[1] The minimum energy path (MEP) connecting the stationary points may be calculated by various methods,[2–6] and the reaction valley may be described by 3N-7 vibrational modes orthogonal to the MEP.[7,8] The method of determining these vibrations may be seen as a conventional vibrational analysis after projecting the gradient out of the force constant matrix.[7–9] A key position in this investigation is the evaluation of the generalized normal mode frequencies ω_i as a function of s, where s is the reaction coordinate (s equals 0 at the transition state, $s < 0$ at the educt side, and $s > 0$ at the product side of the reaction).[8,10] The 3N-7 generalized frequencies may undergo some crossings and avoided crossings when following a chemical reaction, depending on the electronic structure and symmetry of the molecule along the reaction path. As the force

constant matrix is evaluated only at some points along the reaction path, the correct ordering of the normal modes between the discrete steps along the MEP is a nontrivial but important task. The importance of the reordering of normal modes lies in the dependence of the coupling coefficients $B_{i,s}(s)$[10] on the right assignment. With the help of coupling, one can determine if and how the normal modes couple with the reaction coordinate and therefore how they contribute to the progress of the reaction at each stage. Further on a unified reaction valley analysis may be performed properly, which is a powerful tool for a thorough investigation of a chemical reaction.[11] In addition to that the widely used small curvature tunneling correction is determined with the help of the $B_{i,s}(s)$.[8,10,12–16]

In the easiest case the mode reordering is carried out by symmetry requirements to detect avoided crossings of the $\omega_i(s)$

---

directly. If the reaction is of C_1-symmetry or if the symmetry changes along a reaction path (thus leading to bifurcation points[17]) the reordering might become a difficult task. Even if the system is theoretically of a certain symmetry throughout the reaction, there are still numerical inaccuracies in determining the MEP, which might distort the symmetry. Normally this does not affect the whole investigation but forces the reduction of the step size along the MEP, which leads to considerable computational effort. The advantages of the new reordering algorithm over former reordering procedures have already been discussed by Konkoli et al.,[18] and a very consistent algorithm for adiabatic mode ordering was proposed. We use this algorithm as a basis and present improvements that allow a bigger step size along the MEP and assure the correct reordering of the normal modes; we also do this in the cases where the algorithm by Konkoli et al.[18] fails for numerical reasons. One should be aware that there are also other definitions of reaction paths in the literature[3] where this mode reordering might be applied as well. The choice of the MEP as reaction path is straightforward, as it is also used in reaction valley studies.[11]

Short Overview of Mode Reordering

As the theory of mode reordering can be found elsewhere very elaborately,[18] we just want to give a brief overview about the key features: The force constant matrix is determined in internal mass weighted coordinates at some points along the MEP and at the stationary points. On the nonstationary points the gradient is projected out to determine the generalized normal modes along the reaction path.[7,9] From the projected force constant matrices one calculates the eigenvalues and eigenvectors, which are proportional to the square of the frequencies ω_i and equal to the normal modes a_i, respectively.[19] Then the space spanned by the eigenvectors at each point is partitioned into subspaces according to the symmetry of the molecule and the degeneracy of the normal modes. On neighboring points the eigenvectors are rotated to maximize the overlap (scalar product) between the normal modes. Thus the eigenvalues associated with the eigenvectors yielding the largest overlap on neighboring points are assigned to each other.

This way of mode reordering is adiabatic, as one uses the eigenvectors of the projected force constant matrix to gain correct mode assignments. A diabatic treatment involves modes that do not necessarily diagonalize the projected force constant matrix.[20,21] We don't want to adopt this small inconsistency from Konkoli et al., and thus we call our algorithm "Adiabatic Mode Reordering."

Numerical Problems within the Method

The algorithm by Konkoli et al.[18] treats the whole problem very satisfyingly in theory. When evaluating the numerical stability of all subsequent steps one realizes that there might occur problematic situations in the determination of the eigenvectors (i.e., the normal modes). When considering a mode-crossing of, for example, two normal modes, the two eigenvectors span a two-dimensional invariant subspace that has an infinite number of eigenvector bases. One may surmise that the eigenvectors already begin to become undetermined when the eigenvalues begin to coalesce.[22]

Example in Two Dimensions

As an example for this indeterminateness we chose a symmetric two by two matrix, which depends on a parameter x:

$$\mathbf{T}(x) = \begin{pmatrix} 1 + \dfrac{x}{1000} & -\dfrac{1}{10000} \\ -\dfrac{1}{10000} & 1 - \dfrac{x}{1000} \end{pmatrix} \tag{1}$$

The eigenvalues of matrix $\mathbf{T}(x)$ are depicted in Figure 1 and they show an avoided crossing at $x = 0$. The aim now is to determine the maximal overlap between neighboring eigenvectors when changing the parameter x with a finite step size. One has different possibilities to solve this problem. Either one determines the matrix at each step and evaluates the eigenvectors numerically, or an analytic expression for the angle is derived. Appendix I gives the formulas for the analytic expression for the eigenvalues and the eigenvectors, and the formula for the angle between the eigenvectors at neighboring points. The stepsize is chosen $t = 0.02$ and the matrices are calculated for $-0.8 \le x \le 0.8$. The eigenvectors are determined numerically with the QR-method[22] with the help of the program MATLAB.[23] Figure 1 also shows the angles enclosed by the eigenvectors at neighboring points for the numerical evaluated eigenvectors. The angles are compared to the ones derived by the analytical formula [eq. (10), Appendix I], and one sees clearly that the numerical angles deviate strongly from the analytical ones when the two eigenvalues approach each other.

The angle derived by analytical means has its maximum at around 5° and the numerically calculated neighbored eigenvectors enclose angles of more than 30°. If one enlarges the step size, the numerical angle even reaches a value of 45°, which means that no useful assignment can be done, either to eigenvector 1 or to eigenvector 2 at the next point, as there is the same overlap with both of them. In this article we will show the reason for this wobbliness of the eigenvectors associated with nearby eigenvalues in the framework of a perturbative approach, and we will give some proposals for improvement of the original algorithm.

Perturbation Theory of Eigenvalues and Eigenvectors

One has to bear in mind that the theoretical investigation about the eigenvalues and eigenvectors is directly coupled to chemical and spectroscopic features, as the eigenvectors of the projected force constant matrix correspond to the generalized normal modes, and the frequencies are proportional to the square root of the eigenvalues. To see the source of the numerical problems of determining the eigenvectors one has to investigate their behavior by perturbation theory. When stepping from one point to the neighboring one, the projected matrix of second derivatives changes from $\mathbf{F}(s)$ to $\mathbf{F}(s + t)$ (with s being the length parameter along the reaction path, and t being the finite step size). If t is small, the change in $\mathbf{F}(s)$ is also small. (We define $E := \mathbf{F}(s + t) - \mathbf{F}(s)$ as a small perturbation matrix.) According to the theorem of *Wielandt-Hoffmann* the changes in the eigenvalues are also small[22,24]:
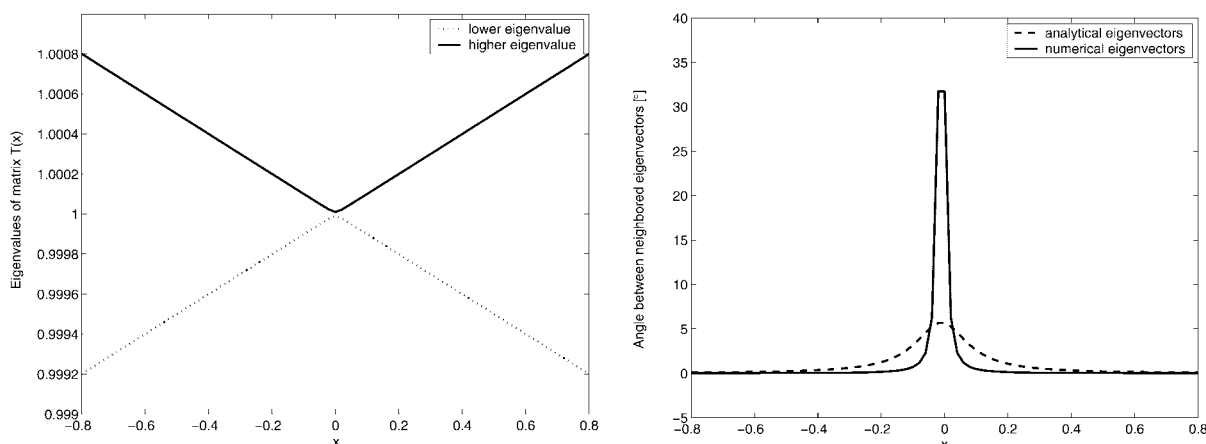
Figure 1. Left: The eigenvalues of the matrix $\mathbf{T}(x)$ in dependence of x. One sees an avoided crossing at $x = 0$. Right: The angles between the eigenvector 1 at two neighboring points with a distance $t = 0.02$. When calculated analytically no big changes in the direction are found, but when deriving the eigenvector numerically big uncertainties appear at $x = 0$.

$$\sum_{i=1}^{n} (\lambda_i(\mathbf{F}(s) + \mathbf{E}) - \lambda_i(\mathbf{F}(s)))^2 \leq \|\mathbf{E}\|_F^2 \qquad (2)$$

λ_i is the i-tallest eigenvalue of the according matrix, n the dimension of the square matrix $\mathbf{F}$, and $\| \cdot \|_F$ defines the Frobenius norm. One has to bear in mind that this applies only to symmetric matrices and symmetric perturbations, which are much more well-behaved than nonsymmetric ones because the condition of the eigenvalues equals 1.[22] From eq. (2) one can conclude that there are no numerical difficulties in the perturbational expansion of the eigenvalues if the perturbation $\mathbf{E}$ is sufficiently small.

Perturbation of the Eigenvalues

If λ_k is a single eigenvalue of the symmetric matrix $\mathbf{F}$ and $\mathbf{E}$ is a symmetric perturbation with $\|\mathbf{E}\|_2 = 1$ one can deduce for $\lambda_k(\varepsilon)$, which is the corresponding eigenvalue of $(\mathbf{F} + \varepsilon\mathbf{E})$

$$\lambda_k(\varepsilon) = \lambda_k + c_1\varepsilon + c_2\varepsilon^2 + c_3\varepsilon^3 + O(\varepsilon^4) \qquad (3)$$

with $\quad c_1 = b_{kk}$

$$c_2 = \sum_{i \neq k}^{n} \frac{b_{ki}^2}{\lambda_k - \lambda_i}$$

$$c_3 = \sum_{i \neq k}^{n} \frac{b_{ki}}{\lambda_i - \lambda_k} \left(\frac{b_{kk}b_{ki}}{\lambda_k - \lambda_i} - \sum_{j \neq k}^{n} \frac{b_{kj}b_{ij}}{\lambda_k - \lambda_j} \right)$$

The b_{ij} are defined as $b_{ij} = x_i^T \mathbf{E} x_j$, when x_i is the eigenvector of $\mathbf{F}$ corresponding to the eigenvalue λ_i, and $(\cdot)^T$ is used to denote the transpose of a matrix. The principle of the derivation is found in Appendix II.

Perturbation of the Eigenvectors

If the conditions of the last section hold, the eigenvector $x_k(\varepsilon)$ corresponding to the eigenvalue $\lambda_k(\varepsilon)$ can be expressed as

$$x_k(\varepsilon) = x_k + d_1\varepsilon + d_2\varepsilon^2 + O(\varepsilon^3) \qquad (4)$$

with $\quad d_1 = \sum_{i \neq k}^{n} \frac{b_{ki}}{\lambda_k - \lambda_i} x_i$

$$d_2 = \sum_{j \neq k}^{n} \frac{1}{\lambda_j - \lambda_k} \left(\frac{b_{kk}b_{kj}}{\lambda_k - \lambda_j} - \sum_{i \neq k}^{n} \frac{b_{ji}b_{ik}}{\lambda_k - \lambda_i} \right) x_j$$

The perturbation of first order of eq. (3) has already been reported in literature,[22,24] whereas the perturbations of higher order or the complete perturbational approach of the eigenvectors is derived on our own. [One has to keep in mind that the resulting vector $x_k(\varepsilon)$ has to be normalized.]

Practical Meaning

When comparing eqs. (3) and (4) it becomes apparent that the eigenvectors show a much higher sensitivity to a small perturbation when some eigenvalues stick close together. For eigenvalues the perturbation of first order (c_1) is independent of the separation of the eigenvalues. In comparison, the first order perturbation of the eigenvectors (d_1) has a term $\lambda_k - \lambda_i$ in the denominator so that d_1 becomes very big when eigenvalues λ_i approach the associated eigenvalue λ_k. This can explain the findings of the section Example in Two Dimensions, as the associated eigenvectors become more and more undetermined when the eigenvalues approach each other.

This has some consequences for the mode reordering algorithm, because the overlap-method is now shown to fail if eigenvalues approach each other. In the next section an extension to the original algorithm by Konkoli et al.[18] is presented. This extension
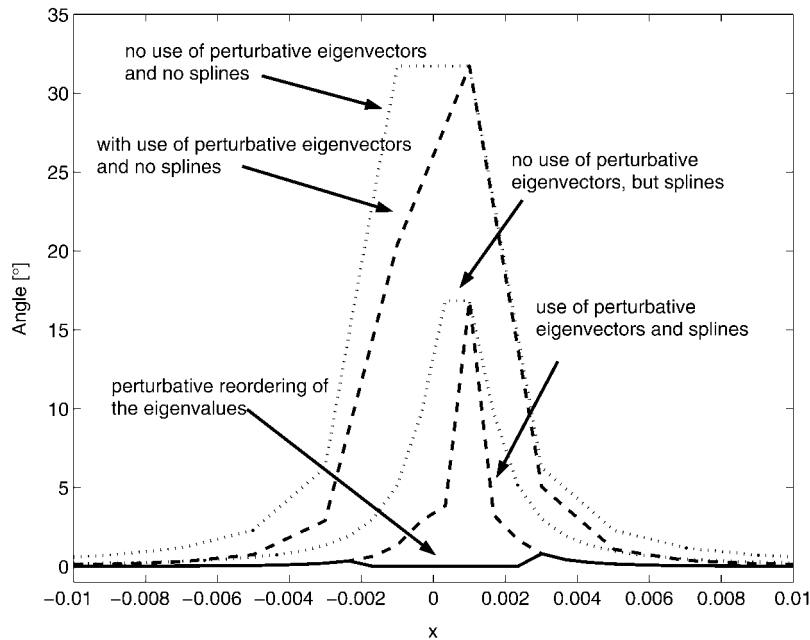
Figure 2. Angle between eigenvectors at neighboring points from the example from the section Example in Two Dimensions and Figure 1. Comparison of the different improvements of the original algorithm (which is labeled as "no use of perturbative eigenvectors and no splines") show that all modifications lead to an obvious improvement of the overlap.

circumvents the numerical problems introduced by the sensitivity of eigenvectors and allows larger stepsizes along the MEP, which lowers the cost of the whole computation.

Implementation into the Algorithm

The new algorithm is a modification of the original one[18] with two changes: The first extension is due to the perturbational approach and affects the reordering of close modes, and the second change is a better interpolation scheme to create intermediate points of the force constant matrix. At this point one should mention that the choice of the coordinate system is of big importance. Internal curvilinear coordinates[25] provide a physically more accurate description of the system than the rectilinear ones.

Perturbational Reordering

From the perturbational approach in the sections Perturbation of the Eigenvalues and Perturbation of the Eigenvectors, two results can be used for an extension of the original algorithm.

The apparent use of the perturbational results is the possibility of calculating the overlap between the perturbed eigenvector at the recent point and the eigenvector of the next point. In the original algorithm[18] the overlap $\mathbf{S}_{AB}$ between the neighboring eigenvectors a and b is generated via Formula (21), and the new access changes this to

$$(\mathbf{S}_{AB})_{\mu\nu} = \left(a_\mu + \sum_{k \neq \mu}^{n} \frac{f_{\mu,k}}{\lambda_\mu - \lambda_k} a_k + \cdots \right)^T b_\nu \qquad (5)$$

with $f_{\mu,k} = a_\mu^T \mathbf{E} a_k$ and a_i being the eigenvectors of the force constant matrix $\mathbf{F}$. $\mathbf{E}$ is the previously defined small perturbation in the force constant matrix: $\mathbf{E} = \mathbf{F}(s + t) - \mathbf{F}(s)$.

This is a direct consequence from eq. (4) and one can decide whether to include the perturbation of first or even second order. Experiments with various examples have shown that first order is usually sufficient. Figure 2 shows that the use of perturbed eigenvectors leads to a significant decrease in the angle between neighbors, although the maximal angle stays the same. Thus it is obvious that although the use of perturbed eigenvectors improves the situation by increasing the overlap, the numerical uncertainty in the eigenvectors associated with close eigenvalues still remains. Therefore there is need of a special treatment for exactly these situations when the overlap is still small although perturbed eigenvectors are used.

As it was shown, the eigenvectors are of no use close to (avoided) crossings of the associated eigenvalues, thus the modification of the algorithm must rely on the eigenvalues and their perturbations. The idea is to predict the propagations of close eigenvalues after the next step and compare the predicted values with the calculated eigenvalues at this neighboring point.

The progressions of an eigenvalue λ_μ may be deduced from eq. (3) as
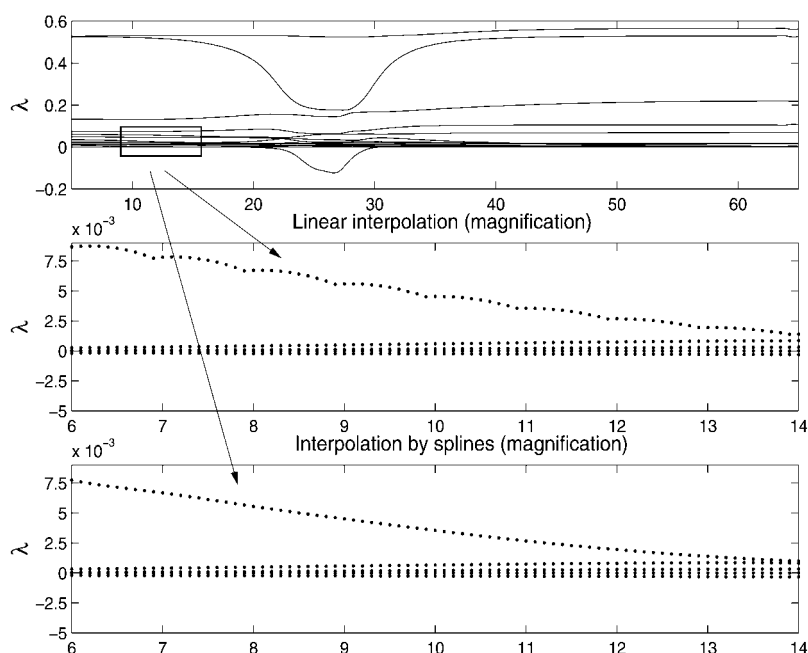
Figure 3. Top: The eigenvalues along the MEP of the decomposition reaction of carbonic acid ($H_2CO_3 \rightarrow H_2O + CO_2$). Middle: A linear interpolation scheme was applied to generate nine additional interpolated force constant matrices between each quantum chemically derived one. A part of the top picture is magnified to show the waving behavior. Bottom: same as the middle picture, but the interpolation was done by cubic splines.

$$\lambda_\mu(s + t) = \lambda_\mu(s) + f_{\mu\mu} + \sum_{k \neq \mu}^{n} \frac{f^2_{\mu,k}}{\lambda_\mu - \lambda_k} + \cdots \qquad (6)$$

The second order perturbation term is of use if $\mathbf{E}$ is small as the term scales with $\|\mathbf{E}\|^2$. The norm of the perturbation may be varied by adjusting the step size, but in all investigated examples, the second order perturbation was very useful. For the eventual case that the second order term is close to singularity one may only consider the first order perturbation. For higher precision and certainty one may even include the third order perturbation into eq. (6), but the result does not improve sufficiently compared to the computational cost in all our investigations.

The proposed procedure for the correct reordering of eigenvalues works as follows:

1. Defining a threshold d. (If two eigenvalues get closer than distance d, the overlap procedure is assumed not to be reliable.)
2. Checking whether two or more eigenvalues come closer than distance d. This yields the set $\Lambda = \{\lambda_i(s) | \exists \lambda_j(s) : |\lambda_i(s) - \lambda_j(s)| \leq d, \text{ with } i \neq j\}$.
3. All eigenvalues $\lambda_k(s) \notin \Lambda$ get reordered by the overlap algorithm, which is similar to the original one by Konkoli et al.,[18] with the extension of first order perturbed eigenvectors.
4. For all eigenvalues $\lambda_k(s) \in \Lambda$ calculate the second order perturbed propagation with eq. (6). This yields a set of perturbed eigenvalues $\lambda_k^p(s)$. Compare the perturbed eigenvalues with the remaining eig-

envalues $\lambda_i(s + t)$ and assign in a way that

$$\sum_{k | \lambda_k(s) \in \Lambda} |\lambda_k^p(s) - \lambda_i(s + t)| \rightarrow \min \qquad (7)$$

This is in general a nontrivial minimization problem, but in the case of vibrational mode reordering just a few (mostly two) modes coincide, so that the global minimization problem is split into some trivial problems.

Figure 2 shows the benefit of the procedure described above. A threshold of $d = 0.0001$ was defined and this prevents application of the overlap procedure if the overlap is not very close to 1. (In the regions where the overlap algorithm couldn't be applied because the eigenvalues were too close to each other, the overlap was explicitly set to 1, i.e., the angle was set to 0°.) Therefore, the new extension of the algorithm combines the advantages of the algorithm by Konkoli et al. in the regions where the eigenvalues are well separated with the new insights about perturbational reordering.

Interpolation by Splines

The matrix elements of the force constant matrix are calculated at each step along the MEP. In the algorithm by Konkoli et al.,[18] linear interpolation between the matrix elements was proposed to yield new points between the quantum chemically determined ones to increase accuracy.[18]

We have found that the linear interpolation scheme leads to misbehavior of the eigenvalues, which can be seen in Figure 3. The
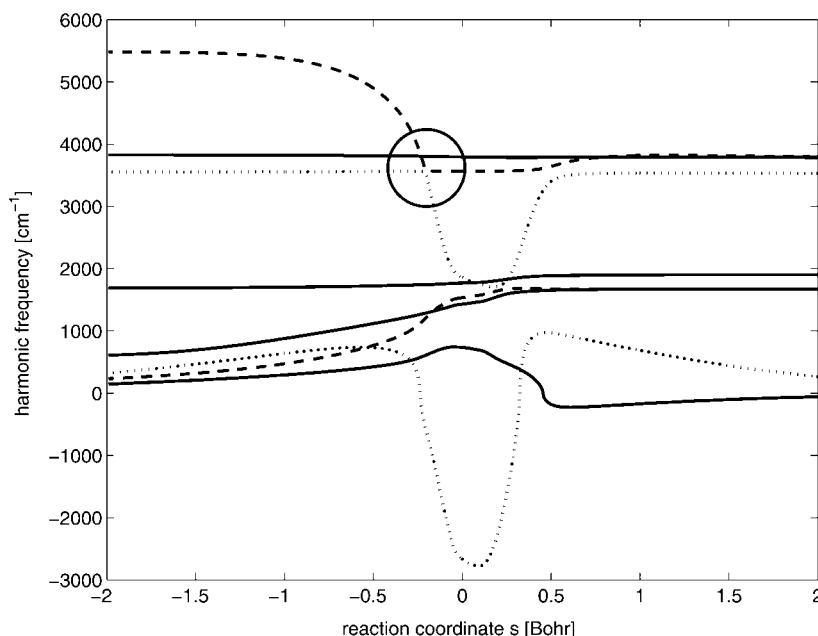
Figure 4. Representation of harmonic frequencies along the MEP in the $CH_3 + H_2 \rightarrow CH_4 + H$ reaction at the UHF/STO-3G level of theory. The stepsize along the reaction path was chosen as 0.05 bohr and the reaction coordinate equals zero at the transition state. The reordering was performed by the new algorithm and an avoided crossing (circle) was resolved, which was not resolved by Konkoli et al. using the same stepsize at the same level of theory.

figure shows the modes along the MEP in the decomposition reaction of carbonic acid ($H_2CO_3 \rightarrow H_2O + CO_2$).[26] The stepsize along the MEP was set to 0.15 bohr, and to get new intermediate points of the force constant matrix, two interpolation schemes have been applied. The linear interpolation leads to very strange features in the behavior of some eigenvalues (Fig. 3, middle picture), as they seem to wave up and down. When performing the interpolation by splines of third order (Fig. 3, bottom picture), the eigenvalue curves are smooth and no evident errors can be found any more. Thus we propose the interpolation by cubic splines to be of better use for generating intermediate points of the projected force constant matrix, rather than linear interpolation. Also, Figure 2 shows the advantages of interpolated points as the maximal angle decreases by a factor of two. Nevertheless, there is still uncertainty in the eigenvectors and the (avoided) crossing at $x = 0$ must be resolved with a perturbational reorder approach. At this point one should mention that interpolation of the second derivative matrix is one, but not the only, possibility to increase the number of points along the MEP. Other approaches include various interpolation schemes[27,28] of the MEP geometries, thus increasing the number of geometries along the MEP.
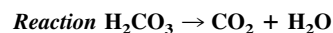
## Application of the Extended Mode Reordering Method

Reaction $CH_3 + H_2 \rightarrow CH_4 + H$
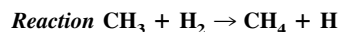
To directly compare the algorithms we examined the reaction $CH_3 + H_2 \rightarrow CH_4 + H$ at the UHF/STO-3G level of theory as was

originally done by Konkoli et al. Although there have been many detailed investigations of this reaction[29,30] or directly related ones,[31] also at much higher level of theory,[11,30,32] we decided to use this level of theory and this reaction to study the advantages of the improvements of the algorithm under the same conditions. The quantum chemical calculations were performed by using GAUSSIAN98[33] and the reaction path was determined with POLYRATE[34] and GAUSSRATE,[35] which is the interface between GAUSSIAN98 and POLYRATE.

Figure 4 shows a plot of the already reordered harmonic vibrations of the mentioned reaction, where the stepsize along the MEP was chosen as 0.05 bohr. An avoided crossing (circle) could be resolved with the new method, which was not resolved with the old algorithm, using the same stepsize along the MEP. All supplementary information about this reaction (e.g., vibrational assignments) may be found elsewhere.[11] The main point is that under the same conditions the improved algorithm shows a correct behavior, where the original algorithm suffered from numerical problems. The time saved may be enormous—in this case the step size was chosen to be five times larger than in the algorithm by Konkoli et al.,[18] to yield a correct mode assignment. Thus, the computational cost was reduced to a fifth (from 1609 s to 337 s on a Pentium 2 GHz for calculating the MEP from -2.5 to $+2.5$ bohr).

Reaction $H_2CO_3 \rightarrow CO_2 + H_2O$

The most useful application of the improved algorithm lies in the reordering of frequencies in reactions of C_1-symmetry, as there are no symmetry constraints, which forces analytical mode reordering.
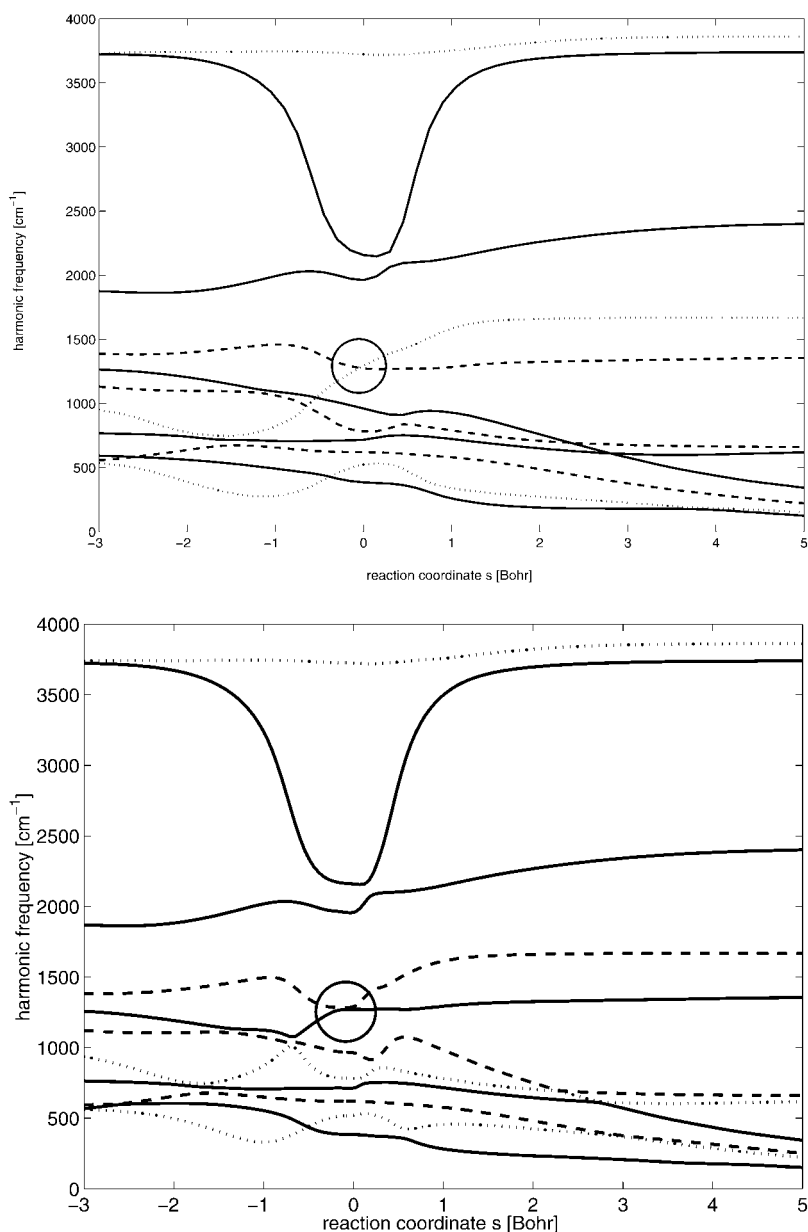
Figure 5. Top: The generalized normal mode frequencies of the decomposition reaction of carbonic acid ($H_2CO_3 \rightarrow CO_2 + H_2O$), reordered by the old algorithm.[18] Bottom: Same as in the upper picture, but the reordering was done with the new extensions of the algorithm. The nature of some crossings changed completely, as an example the marked (avoided) crossing will be examined in detail.

Thus we used the decomposition reaction of carbonic acid to water and carbon dioxide as an example to test the performance of the new algorithm. The MEP was determined at a B3LYP/6-31+G(d) level of theory and a stepsize of 0.05 bohr (with the same program packages as in the last section). Second derivatives were calculated every third step, so that generalized normal mode analysis was performed every 0.15 bohr. Figure 5 shows the generalized normal mode frequencies, once reordered with the old algorithm, and once with the new, improved version. One clear difference between the two methods lies in the resolution of various crossings. One differently resolved crossing was chosen as an example (marked by the circle at $s = -0.15$) to decide which algorithm resolved it the right way.

For a thorough investigation of the generalized normal modes, we depicted the modes (drawn as vectors) together with the molecules at the reaction path on both sides of the crossing (Fig. 6). We wanted to decide which algorithm performed correctly by "visual inspection" of the two nearby modes before and after the
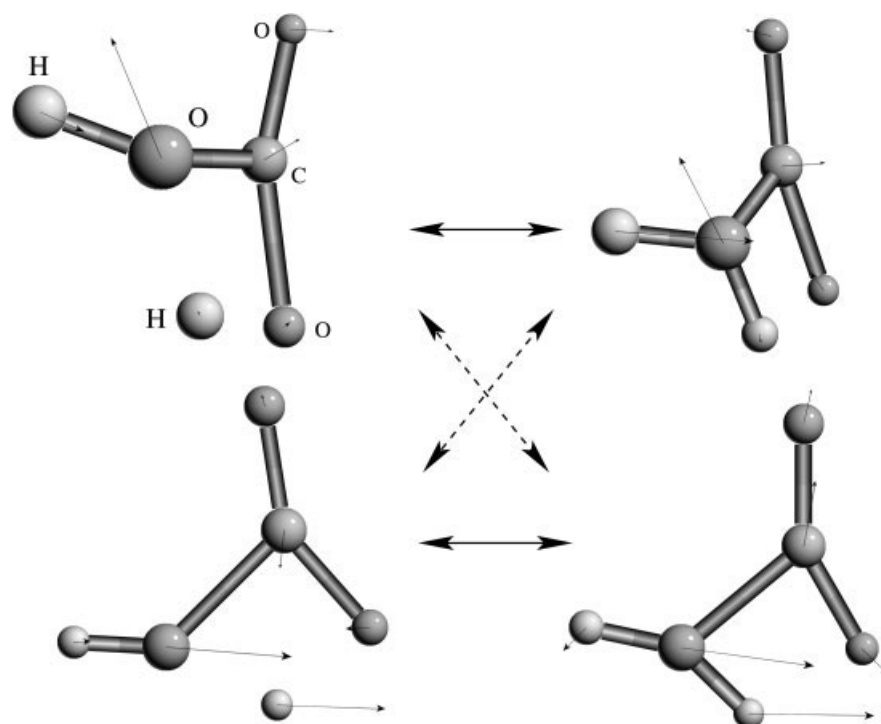
Figure 6. The normal modes before and after the avoided crossing from Figure 5. The top pictures show the normal modes belonging to the higher harmonic frequencies, and the bottom pictures show the normal modes belonging to the lower harmonic frequencies. The correspondence between horizontally neighboring motions can easily be seen (assignment by solid arrows) and therefore it can be followed that an avoided crossing is present. If the assignment followed the dashed arrows, a real crossing would have occurred.

crossing. Thus we compared the vibrational motion of the molecule at $s = -0.3$ and with a frequency of 1292 cm^{-1} (upper left picture in Fig. 6) with the two possible propagations at $s = 0.0$ with the frequencies 1295 and 1272 cm^{-1} (upper right and lower right picture in Fig. 6, respectively). One may find a clear correspondence between the two upper pictures and between the two lower pictures, as the generalized normal mode vectors have similar directions. Therefore one may surmise that the higher frequency before the (avoided) crossing can be matched to the higher frequency after the (avoided) crossing, thus really causing an avoided crossing. This is only one example of different resolution of crossings by the two algorithms. There may be many more found when looking at Figure 5, thus emphasizing the big difference in the performance of the original and the improved algorithm.

Conclusions

The algorithm for reordering of normal modes by Konkoli et al.,[18] although being analytically very useful, has been shown to suffer from numerical problems, especially when two harmonic frequencies approach each other. We propose an extension of the original algorithm on the one hand by a more powerful interpolation procedure of the projected force constant matrix, which makes use of cubic splines instead of linear interpolation. On the other hand we have stressed the numerical instability of the original algorithm, and we propose circumvention of these problems by perturbational approaches to both the eigenvalues and eigenvectors of the force constant matrix. These values correspond proportionally to the square of the harmonic frequencies and the normal modes of a molecule, respectively. The new algorithm improves reordering of the frequencies twofold: First, a larger stepsize along the minimum energy path can be chosen, thus reducing the computational effort considerably. Second, the resolution of the crossings has been shown to be more reliable with the improved algorithm.

One more benefit of this work is that the perturbational approach exhibits the big problems that appear when working with eigenvectors belonging to nearby eigenvalues. The direction of the eigenvectors becomes undetermined and they are of no physical meaning for any useful quantitative analysis. Thus one has to bear in mind that this result does not only affect the reordering of normal modes, but all situations in physical and chemical systems, when eigenvector analysis is performed on experimental data.

Appendix I

The eigenvalues and eigenvectors of matrix $T(x)$ can easily be derived with a computer algebra package[36] as

$$_2\text{Eval}_1 = 1 \pm \frac{\sqrt{1 + 100x^2}}{10000} \tag{8}$$

and

$$_2\text{Evec}_1 = \begin{pmatrix} -10x \mp \sqrt{1 + 100x^2} \\ 1 \end{pmatrix} \tag{9}$$

respectively.

Thus, having defined a stepsize t between discrete values of x, one has to evaluate the angle between the eigenvectors $\text{Evec}_1(x)$ and $\text{Evec}_1(x + t)$, which turns out to be

$$\text{acos} \frac{(-10x - \sqrt{1 + 100x^2})(-10x - 10t - \sqrt{1 + 100x^2 + 200xt + 100t^2 + 1})}{\sqrt{(-10x - \sqrt{1 + 100x^2})^2 + 1} \sqrt{(-10x - 10t - \sqrt{1 + 100x^2 + 200xt + 100t^2 + 1})^2 + 1}} \tag{10}$$

Appendix II

First, let's recall some properties of eigenvalues and eigenvectors of symmetric matrices:

- A matrix $\mathbf{A} \in \mathbb{R}^{n \times n}$ is called symmetric if $\mathbf{A}^T = \mathbf{A}$ holds. Thus each symmetric matrix is square.
- The eigenvalues of a symmetric matrix are real.
- Corresponding left and right eigenvectors are identical. They form a set of orthonormal vectors and a basis of $\mathbb{R}^n$.

These statements can be directly deduced from the spectral theorem[37] and will be used here without further justification.

As the second derivative matrix of the energy with respect to the coordinates is evidently symmetric, we can use these properties of the eigenvalues and eigenvectors.

Expansions of Eigenvectors and Eigenvalues

If $\mathbf{A} \in \mathbb{R}^{n \times n}$ is symmetric and λ_k and x_k are the eigenvalues and eigenvectors, respectively, the following equations hold:

$$\mathbf{A}x_k = \lambda_k x_k$$

$$x_k^T \mathbf{A} = \lambda_k x_k^T \tag{11}$$

When perturbing $\mathbf{A}$ with a symmetric matrix of norm ε, the eigenvalues and eigenvectors are perturbed as well. If ε is sufficiently small, the change in the eigenvalues will also be small [eq. (2)]. For the perturbed quantities the following equations hold:

$$(\mathbf{A} + \varepsilon\mathbf{E})x_k(\varepsilon) = \lambda_k(\varepsilon)x_k(\varepsilon)$$

$$x_k(\varepsilon)^T(\mathbf{A} + \varepsilon\mathbf{E}) = \lambda_k(\varepsilon)x_k(\varepsilon)^T \tag{12}$$

E is a symmetric perturbation with $\|\mathbf{E}\| = 1$, so that $\|\varepsilon E\| = \varepsilon$.

The eigenvalues $\lambda_k(\varepsilon)$ and the associated eigenvectors $x_k(\varepsilon)$ may be expanded in power series:

$$\lambda_k(\varepsilon) = \lambda_k + c_1\varepsilon + c_2\varepsilon^2 + O(\varepsilon^3) \tag{13}$$

$$x_k(\varepsilon) = x_k + d_1\varepsilon + d_2\varepsilon^2 + O(\varepsilon^3) \tag{14}$$

where $d_i \in \mathbb{R}^n$ and $c_i \in \mathbb{R}$. As the eigenvectors span the whole $\mathbb{R}^n$, the d_i may be represented on the basis of the eigenvectors x_j:

$$d_i = \sum_{j=1}^n s_{ij}x_j \tag{15}$$

Inserting expansions (13) and (14) into eq. (12) and substituting the d_i via eq. (15) yields

$$(\mathbf{A} + \varepsilon\mathbf{E})\left(x_k + \varepsilon \sum_{j=1}^n s_{1j}x_j + \varepsilon^2 \sum_{j=1}^n s_{2j}x_j + \cdots\right)$$

$$= (\lambda_k + c_1\varepsilon + c_2\varepsilon^2 + \cdots)$$

$$\times \left(x_k + \varepsilon \sum_{j=1}^n s_{1j}x_j + \varepsilon^2 \sum_{j=1}^n s_{2j}x_j + \cdots\right) \tag{16}$$

By the method of coefficient comparison of the ε^1-terms, eq. (16) yields

$$\mathbf{A} \sum_{j=1}^n s_{1j}x_j + \mathbf{E}x_k = \lambda_k \sum_{j=1}^n s_{1j}x_j + c_1x_k \tag{17}$$

and coefficient comparison of the ε^2-terms results in

$$\mathbf{A} \sum_{j=1}^n s_{2j}x_j + \mathbf{E} \sum_{j=1}^n s_{1j}x_j = \lambda_k \sum_{j=1}^n s_{2j}x_j + c_1 \sum_{j=1}^n s_{1j}x_j + c_2 \tag{18}$$

Recalling eq. (11), eq. (17) may be transformed into

$$\sum_{j=1}^{n} (\lambda_j - \lambda_k)s_{1j}x_j + \mathbf{E}x_k = c_1 x_k \tag{19}$$

When multiplying eq. (19) from the left with x_i^T ($i = 1, \ldots, n$) one has to discriminate between two cases:

- Case 1: $i = k$

  The whole sum on the left hand side of eq. (19) becomes zero (because of the orthonormality of the eigenvectors of **A**) and eq. (19) becomes

  $$x_k^T \mathbf{E} x_k = c_1 \tag{20}$$

  which is exactly the result presented in eq. (3) for the perturbation of first order of the eigenvalues.

- Case 2: $i \neq k$

  Eq. (19) becomes

  $$(\lambda_i - \lambda_k)s_{1i} + x_i^T \mathbf{E} x_k = 0$$

  thus yielding

  $$s_{1i} = \frac{x_i^T \mathbf{E} x_k}{\lambda_k - \lambda_i} \tag{21}$$

  and therefore

  $$d_1 = \sum_{i \neq k}^{n} \frac{x_i^T \mathbf{E} x_k}{\lambda_k - \lambda_i} x_i \tag{22}$$

  which is exactly the result presented in eq. (4) for the perturbation of first order of the eigenvectors.

In a similar manner one may deduce the second order perturbations from eq. (18), and even higher order perturbations when collecting terms in eq. (16) that are of higher order in ε. As the calculations are analogous, they will be omitted.

References

1. Jensen, F. Introduction to Computational Chemistry; John Wiley & Sons: Chichester, England, 1999; Chapter 13.
2. Page, M.; McIver, J. W. J Chem Phys 1988, 88, 922.
3. Gonzales, C.; Schlegel, H. B. J Chem Phys 1989, 90, 2154.
4. Gonzalez, C.; Schlegel, H. B. J Phys Chem 1990, 94, 5523.
5. Gonzalez, C.; Schlegel, H. B. J Chem Phys 1991, 95, 5853.
6. Melissas, V. S.; Truhlar, D. G.; Garrett, B. C. J Chem Phys 1992, 96, 5758.
7. Miller, W. H.; Handy, N. C.; Adams, J. E. J Chem Phys 1980, 72, 99.
8. Tucker, S. C.; Truhlar, D. G. In New Theoretical Concepts for Understanding Organic Reactions; Bertran, J., Csizmadia, I. G., Ed.; Kluwer Academic Publishers: Dordrecht, The Netherlands, 1989; p 291.
9. Baboul, A. G.; Schlegel, H. B. J Chem Phys 1997, 107, 9413.
10. Truhlar, D. G.; Isaacson, A. D.; Garrett, B. C. In Theory of Chemical Reaction Dynamics; Baer, M., Ed.; CRC Press: Boca Raton, FL, 1985; p 65.
11. Konkoli, Z.; Kraka, E.; Cremer, D. J Phys Chem A 1997, 101, 1742.
12. Marcus, R. A.; Coltrin, E. J Chem Phys 1977, 67, 2609.
13. Skodje, R. T.; Truhlar, D. G.; Garret, B. C. J Phys Chem 1981, 85, 3019.
14. Skodje, R. T.; Truhlar, D. J Chem Phys 1982, 77, 5955.
15. Lu, D.-h.; Truong, T. N.; Melissas, V. S.; Lynch, G. C.; Liu, Y.-P.; Garrett, B. C.; Steckler, R.; Isaacson, A. D.; Rai, S. N.; Hancock, G. C.; Lauderdale, J. G.; Joseph, T.; Truhlar, D. G. Comput Phys Commun 1992, 71, 235.
16. Liu, Y.-P.; Lynch, G. C.; Truong, T. N.; Lu, D.-h.; Truhlar, D. G.; Garrett, B. C. J Am Chem Soc 1993, 115, 2408.
17. Quapp, W.; Hirsch, M.; Imig, O.; Heidrich, D. J Comput Chem 1998, 19, 1087.
18. Konkoli, Z.; Cremer, D.; Kraka, E. J Comput Chem 1997, 18, 1282.
19. Primas, H.; Müller-Herold, U. Elementare Quantenchemie; Teubner Studienbücher: Stuttgart, 1980.
20. Truhlar, D. G.; Isaacson, A. D. J Chem Phys 1982, 77, 3516.
21. Sidis, V. In Advances in Chemical Physics, Vol. LXXXII; Baer, M., Ng, C.-Y., Eds.; John Wiley & Sons, Inc.: New York, 1992; p 73.
22. Golub, G. E.; van Loan, C. F. Matrix Computations, 3rd ed.; The Johns Hopkins University Press: Baltimore, MD, 1996.
23. MATLAB, 5.3.1.29215a ed.; High performance numeric computation and visualization software; The MathWorks, Inc.: Natick, MA, 1999.
24. Wilkinson, J. H. The Algebraic Eigenvalue Problem; Oxford University Press: Ely House, London, 1965.
25. Jackels, C. F.; Gu, Z.; Truhlar, D. G. J Chem Phys 1995, 102, 3188.
26. Loerting, T.; Tautermann, C.; Kroemer, R. T.; Kohl, I.; Hallbrucker, A.; Mayer, E.; Liedl, K. R. Angew Chem Int Ed 2000, 39, 891.
27. Corchado, J. C.; Coitiño, E. L.; Chang, Y.-Y.; Fast, P. L.; Truhlar, D. G. J Phys Chem A 1998, 102, 2424.
28. Kim, Y.; Corchado, J. C.; Villà, J.; Xing, J.; Truhlar, D. G. J Chem Phys 2000, 112, 2718.
29. Baldridge, K. K.; Gordon, M. S.; Steckler, R.; Truhlar, D. G. J Phys Chem 1989, 93, 5107.
30. Pu, J.; Truhlar, D. G. J Chem Phys 2002, 116, 1468.
31. Corchado, J. C.; Truhlar, D. G.; Espinosa-García, J. J Chem Phys 2000, 112, 9375.
32. Kurosaki, Y.; Takayanagi, T. Chem Phys Lett 1999, 199, 57.
33. Frisch, M. J.; Trucks, G. W.; Schlegel, H. B.; Scuseria, G. E.; Robb, M. A.; Cheeseman, J. R.; Zakrzewski, V. G.; Montgomery, J. A.; Stratmann, R. E.; Burant, J. C.; Dapprich, S.; Millam, J. M.; Daniels, A. D.; Kudin, K. N.; Strain, M. C.; Farkas, O.; Tomasi, J.; Barone, V.; Cossi, M.; Cammi, R.; Mennucci, B.; Pomelli, C.; Adamo, C.; Clifford, S.; Ochterski, J.; Petersson, G. A.; Ayala, P. Y.; Cui, Q.; Morokuma, K.; Malick, D. K.; Rabuck, A. D.; Raghavachari, K.; Foresman, J. B.; Cioslowski, J.; Ortiz, J. V.; Stefanov, B. B.; Liu, G.; Liashenko, A.; Piskorz, P.; Komaromi, I.; Gomperts, R.; Martin, R. L.; Fox, D. J.; Keith, T.; Al-Laham, M. A.; Peng, C. Y.; Nanayakkara, A.; Gonzalez, C.; Challacombe, M.; Gill, P. M. W.; Johnson, B. G.; Chen, W.; Wong, M. W.; Andres, J. L.; Head-Gordon, M.; Replogle, E. S.; Pople, J. A. GAUSSIAN98, Revision A.7; Gaussian, Inc.: Pittsburgh, PA, 1998.
34. Chuang, Y.-Y.; Corchado, J. C.; Fast, P. L.; Villá, J.; Coitiño, E. L.; Hu, W.-P.; Liu, Y.-P.; Lynch, G. C.; Nguyen, K. A.; Jackels, C. F.; Gu, M. Z.; Rossi, I.; Clayton, S.; Melissas, V. S.; Steckler, R.; Garrett, B. C.; Isaacson, A. D.; Truhlar, D. G. POLYRATE, version 8.5; University of Minnesota: Minneapolis, MN, 2000.
35. Corchado, J. C.; Coitiño, E. L.; Chuang, Y.-Y.; Truhlar, D. G. GAUSSRATE 8.5; University of Minnesota: Minneapolis, MN, 2000.
36. MAPLE, 7th ed.; Waterloo Maple Inc.: Waterloo ON2L6C2, Canada, 2001.
37. Klingenberg, W. Lineare Algebra und Geometrie, 2nd ed.; Springer-Verlag: Berlin, 1992.